Inorganic Chemistry
Cite This: Inorg. Chem. XXXX, XXX, XXX−XXX
Article
pubs.acs.org/IC

MOF-253-Supported Ru Complex for Photocatalytic CO_2 Reduction by Coupling with Semidehydrogenation of 1,2,3,4-Tetrahydroisoquinoline (THIQ)

Xiaoyu Deng, Yuhuan Qin, Mingming Hao, and Zhaohui Li*

Research Institute of Photocatalysis, State Key Laboratory of Photocatalysis on Energy and Environment, College of Chemistry, Fuzhou University, Fuzhou 350116, People's Republic of China

Supporting Information

ABSTRACT: MOF-253 (Al(OH)(dcbpy), dcbpy = 2,2′-bipyridine-5,5′-dicarboxylic acid) obtained via a microwave-assisted synthesis was used for the construction of a supported Ru complex containing dcbpy (MOF-253-Ru(dcbpy)$_2$) by coordinating its open N,N′-chelating sites with Ru(II) in Ru(dcbpy)$_2$Cl$_2$. The as-obtained MOF-253-Ru(dcbpy)$_2$ acts as a bifunctional photocatalyst for simultaneous CO_2 reduction to produce formic acid and CO, as well as semidehydrogenation of 1,2,3,4-tetrahydroisoquinoline (THIQ) to obtain 3,4-dihydroisoquinoline (DHIQ). The performance over the surface-supported MOF-253-Ru(dcbpy)$_2$ is superior to that over Ru-doped MOF-253 (Ru-MOF-253) obtained via a mix-and-match strategy, indicating that the use of open coordination sites in the MOFs for direct construction of a surface-supported complex is a superior strategy to obtain an MOF-supported homogeneous complex. This study shows the possibility of using an MOF as a platform for the construction of multifunctional heterogeneous photocatalytic systems. The coupling of photocatalytic CO_2 reduction with the highly selective dehydrogenation of organics provides an economical and green strategy in photocatalytic CO_2 reduction and production of valuable organics simultaneously.

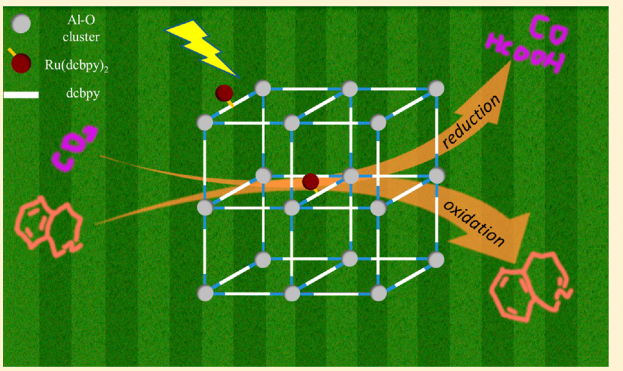

INTRODUCTION

CO_2 is a greenhouse gas, and its increasing concentration in the atmosphere due to an excessive combustion of fossil fuels has caused global warming.[1,2] In comparison with the simple capture and sequestration of CO_2, the use of CO_2 as a chemical feedstock to produce valuable chemicals/fuels via catalytic transformations is a more desirable strategy in treating CO_2, since it can reduce the greenhouse effect while in the meantime relieve the energy shortage pressure.[3−5] In particular, the utilization of the abundant and ubiquitous solar energy for CO_2 reduction to form fuels is extremely appealing.[6,7] However, CO_2 is thermodynamically stable and its conversion to multiple electron reduction products such as CO, HCOOH, CH_3OH, and CH_4 is also kinetically unfavorable, which makes the photocatalytic reduction of CO_2 extremely challenging.[8,9]

Ru complexes containing 2,2′-bipyridine-based diimine ligands have been widely used in photocatalysis.[10,11] In particular, some Ru complexes featuring bpy-based ligands, for example, $[Ru(bpy)_3]Cl_2$ and $Ru(bpy)(CO)_2Cl_2$, have been demonstrated to be photocatalysts for CO_2 reduction to produce CO or formate via proton-coupled reduction pathways.[8,12,13] The proposed mechanism revealed that the excited MLCT state of these Ru complexes can be reductively quenched by sacrificial agents, generally amines and their derivatives, to form the active species for CO_2 reduction.[14] However, the use of sacrificial agents for photocatalytic CO_2 reduction over these Ru-based systems is neither economical nor green, since the oxidation products of these sacrificial agents are usually complicated and cannot be separated from the reaction systems for further applications. A more desirable strategy is to replace the commonly used sacrificial agents by organics that can undergo selective oxidation to form valuable products: i.e., to couple photocatalytic CO_2 reduction with selective oxidation of organics over these Ru-based photocatalysts.

1,2,3,4-Tetrahydroisoquinoline (THIQ), a widely distributed alkaloid in nature, is a good electron donor and a hydrogen source as well.[10,11] Previous studies have revealed that $[Ru(bpy)_3]Cl_2$ is active for the photocatalytic dehydrogenation of THIQ.[15,16] Since $E([Ru(bpy)_3]^{2+*}/[Ru(bpy)_3]^{+})$ (1.07 V vs NHE) is more positive than the first oxidative potential of THIQ (ca. 1.01 V vs NHE), the excited state $[Ru(bpy)_3]^{2+*}$ can be reductively quenched by THIQ to form $[Ru(bpy)_3]^{+}$, together with the generation of 3,4-dihydroisoquinoline (DHIQ), the semidehydrogenation product of THIQ.[17−19] Considering that the as-formed $[Ru(bpy)_3]^{+}$ is

Received: August 27, 2019

DOI: 10.1021/acs.inorgchem.9b02593
Inorg. Chem. XXXX, XXX, XXX−XXX

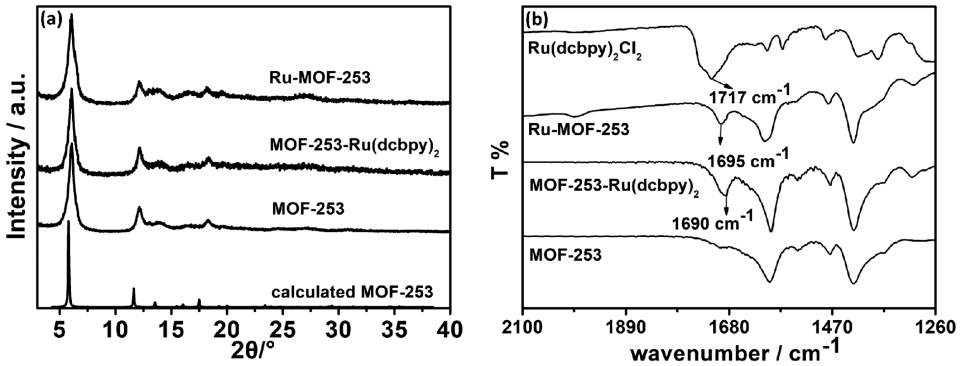

Figure 1. (a) XRD patterns of MOF-253, MOF-253-Ru(dcbpy)$_2$, Ru-MOF-253, and calculated MOF-253. (b) FT-IR spectra of bare MOF-253, MOF-253-Ru(dcbpy)$_2$, Ru-MOF-253, and Ru(dcbpy)$_2$Cl$_2$.

the active species for CO_2 reduction, it is therefore feasible to couple photocatalytic CO_2 reduction with the dehydrogenation of THIQ to produce DHIQ over Ru complexes featuring N,N′-chelating ligands in its structure.[20] Such a coupling reaction is appealing if we consider that DHIQ, the semidehydrogenation product of THIQ, is also an important precursor in the syntheses of pharmaceuticals such as morphinans and isoquinoline alkaloids.[15]

In this paper, we report that simultaneous photocatalytic reduction of CO_2 and semidehydrogenation of THIQ can be realized over an MOF-supported Ru complex containing dcbpy (dcbpy = 2,2′-bipyridine-5,5′-dicarboxylic acid). An obvious advantage of supported molecular catalysts in comparison with their homogeneous counterparts lies in their good recyclability, since they can be facilely separated from the reaction systems.[21,22] As a type of porous material with highly tunable pore structures and well-defined isolated sites for anchoring of catalytic active species, metal−organic frameworks (MOFs) have been demonstrated to be attractive supports for the molecular catalysts.[23−26] In particular, the use of MOF featuring open chelating sites to coordinate with metal ions has been demonstrated to be an ideal strategy to develop stable MOF-supported molecular catalysts without loss of their performance.[27−30] Herein, MOF-253 featuring open N,N′-chelating sites in its structure has been used in the construction of a supported Ru complex containing dcbpy (MOF-253-Ru(dcbpy)$_2$), which simultaneously reduce CO_2 to form CO and formic acid as well as dehydrogenate THIQ to produce DHIQ under visible light.

EXPERIMENTAL SECTION

Preparations. MOF-253 was synthesized from $AlCl_3{\cdot}6H_2O$ and dcbpy in anhydrous DMF via a microwave-assisted heating.[30] $AlCl_3{\cdot}6H_2O$ (602 mg, 2.5 mmol) and dcbpy (611 mg, 2.5 mmol) in DMF (40 mL) were sealed in a 100 mL Teflon liner and heated at 120 °C in a microwave oven (Milestone ETHOS A Microwave Labstation) for 1.5 h. After the reaction, the resultant suspension was filtered, washed with DMF and MeOH, extracted by Soxhlet extraction with MeOH, and vacuum-dried to obtain the white solid product of MOF-253 (555 mg, 77%).

The MOF-253-supported Ru complex was prepared from activated MOF-253 and Ru(dcbpy)$_2$Cl$_2$ solvothermally as shown in Figure S1a in the Supporting Information. Before the reaction, MOF-253 was activated by desolvation under vacuum at 150 °C for 12 h. Ru(dcbpy)$_2$Cl$_2$ was produced according to a method reported previously.[31] MOF-253 (432 mg, 1.5 mmol) and Ru(dcbpy)$_2$Cl$_2$ (100 mg, 0.15 mmol) in anhydrous DMF (15 mL) were sealed in a Teflon liner and heated at 100 °C for 12 h. After the reaction, the suspension was separated by centrifugation, washed with DMF and MeOH, and vacuum-dried to obtain a violet powder (denoted as MOF-253-Ru(dcbpy)$_2$). For comparison, MOF-253 was also obtained by a conventional solvothermal method (denoted as MOF-253-ST), which was used for the construction of the MOF-253-Ru(dcbpy)$_2$ counterpart (denoted as MOF-253-Ru(dcbpy)$_2$-ST).

For comparison, a Ru-doped MOF-253 (denoted as Ru-MOF-253) was also prepared via a mix-and-match strategy developed first by Lin and co-workers with slight modifications by reacting $AlCl_3{\cdot}6H_2O$ with a combination of dcbpy and [Ru(dcbpy)$_3$]Cl$_2$ under microwave heating (shown in Figure S1b in the Supporting Information).[32] [Ru(dcbpy)$_3$]Cl$_2$ was prepared from $RuCl_3{\cdot}3H_2O$ and dcbpy according to a previously reported method.[31] $AlCl_3{\cdot}6H_2O$ (602 mg, 2.5 mmol), dcbpy (549 mg, 2.25 mmol), and [Ru(dcbpy)$_3$]Cl$_2$ (226 mg, 0.25 mmol) in DMF (40 mL) were sealed in a Teflon liner and heated in a microwave oven at 120 °C for 1.5 h. After heating, the resultant suspension was filtered and washed with DMF and MeOH. MOF-253-Ru(CO)$_2$Cl$_2$ was prepared with reference to our previous literature.[14]

Characterizations. The powder X-ray diffraction patterns (XRD) were collected on a Rigaku SmartLab rotation anode X-ray diffractometer with graphite-monochromated Cu Kα radiation. Data were recorded at a scan rate of 0.05° 2θ s^{-1} in the 2θ range from 3 to 60°. The IR spectra were obtained on a Nicolet 670 FT-IR spectrometer. UV−vis diffuse-reflectance spectrometry (UV−vis DRS) were obtained on a UV−visible spectrophotometer (Cary 500 Scan Spectrophotometers, Varian). $BaSO_4$ was used as a reflectance standard. N_2 adsorption/desorption isotherms were obtained on ASAP2020 apparatus (Micromeritics Instrument Corp., USA). The samples were degassed under vacuum at 150 °C for 6 h and measured at 77 K. Inductively coupled optical emission spectrometry (ICP-OES) was performed on an Optima 8000 instrument (PerkinElmer). The X-ray photoelectron spectroscopy (XPS) was performed on a Thermo Scientific ESCALAB 250 XPS system.

Photocatalytic Reactions. Photocatalytic reactions were performed in a sealed Schlenk tube under visible-light irradiation at room temperature. The photocatalyst (10 mg) suspended in MeCN containing THIQ (0.08 mmol) was degassed and saturated with CO_2 before the reaction. The reactions were performed under the irradiation of a 5 W white LED lamp under a CO_2 atmosphere. Gaseous products were analyzed by a GC-FID instrument (Agilent 7890B) equipped with a Ni reformer, a PLOT Q column, and a 5A column, while the liquid products were analyzed by a GC-FID instrument (Shimadzu GC-2014) equipped with a HP-5 capillary column and ion chromatography (881 Compact IC pro, Metrosep) with a Metrosep A supp 5 250/4.0 column. A mixture of 3.2 mM Na_2CO_3 and 1.0 mM $NaHCO_3$ aqueous solutions was used as the eluent. The used photocatalyst was washed several times with MeCN and MeOH and dried for the cycling test.

DOI: 10.1021/acs.inorgchem.9b02593
Inorg. Chem. XXXX, XXX, XXX−XXX

RESULTS AND DISCUSSION

Synthesis and Characterization of MOF-253-Ru-(dcbpy)$_2$. Considering that microwave-assisted heating is more efficient than conventional heating, MOF-253 was prepared from $AlCl_3 \cdot 6H_2O$ and dcbpy via a microwave-assisted method.[30,33] The as-obtained product shows a similar XRD pattern and a slightly larger Langmuir surface area (1632 m^2 g^{-1}) in comparison to that obtained by conventional solvothermal heating (1476 m^2 g^{-1}), indicating that the microwave-assisted method is superior to the conventional solvothermal method in the synthesis of high-quality MOF-253, in particular considering that the reaction time can be reduced from 24 h for conventional heating to 1.5 h for microwave heating (Figure 1a and Figures S2 and S3 in the Supporting Information). To synthesize MOF-253-Ru-(dcbpy)$_2$, the as-obtained MOF-253 was activated and reacted with Ru(dcbpy)$_2$Cl$_2$ in anhydrous DMF at 100 °C under solvothermal conditions (Figure S1a in the Supporting Information). The XRD of the resultant supported MOF-253-Ru(dcbpy)$_2$ shows the characteristic diffraction peaks of MOF-253, suggesting that the framework of MOF-253 is maintained after the coordination of Ru(II) with the open N,N′-chelating sites on dcbpy linkers (Figure 1a). In comparison with that of bare MOF-253, the FT-IR spectrum of MOF-253-Ru(dcbpy)$_2$ shows a new peak at 1690 cm^{-1}, which can be assigned to the stretching vibration of C═O from dcbpy in Ru moieties, indicating the successful introduction of Ru moieties into MOF-253 (Figure 1b). The slight red shift of the C═O vibrational stretch in MOF-253-Ru(dcbpy)$_2$ in comparison with that in homogeneous Ru(dcbpy)$_2$Cl$_2$ clearly indicates the coordination of Ru^{2+} to the N,N′-chelating sites in MOF-253.[34] To provide more evidence for the formation of MOF-253-Ru(dcbpy)$_2$, XPS was also carried out on MOF-253-Ru(dcbpy)$_2$ and MOF-253 (Figure S4 in the Supporting Information). The XPS spectrum of MOF-253-Ru(dcbpy)$_2$ in the Ru 3d region shows a peak at a binding energy of 281.4 eV, assignable to Ru $3d_{5/2}$, although the corresponding Ru $3d_{3/2}$ peak, with its binding energy at ca. 285.6 eV, may be overlapped with that of C 1s. This indicates the existence of Ru^{2+} in MOF-253-Ru(dcbpy)$_2$. In the meantime, the peak corresponding to N 1s in MOF-253-Ru(dcbpy)$_2$ (400.2 eV) shifts by ca. 1.0 eV toward higher binding energy in comparison with that in pristine MOF-253 (399.2 eV), indicating the coordination of the N,N′-open chelating sites in MOF-253 with Ru^{2+} in the as-obtained MOF-253-Ru(dcbpy)$_2$. MOF-253-Ru(dcbpy)$_2$ shows a relatively high Langmuir specific surface area of 1143 m^2 g^{-1}, indicating the maintenance of the permanent porosity (Figure S3a in the Supporting Information). The slight lowering of the specific surface area of MOF-253-Ru(dcbpy)$_2$ in comparison with the pristine MOF-253 (1632 m^2 g^{-1}) can be attributed to the partial occupancy of the pores in MOF-253 by the anchored Ru moieties. The ICP of the digested MOF-253-Ru(dcbpy)$_2$ gave a Ru/Al molar ratio of ca. 6.0 wt %, lower than the Ru/Al ratio (10.0%) in the starting materials, probably due to an incomplete reaction between MOF-253 and Ru(dcbpy)$_2$Cl$_2$ at a relatively low reaction temperature (100 °C), since the reported reaction between dcbpy and $RuCl_3$ to form [Ru(dcbpy)$_3$]Cl$_2$ was carried out at 200 °C.[30,31] All of the characterizations suggest that a MOF-253-supported Ru complex containing dcbpy ligands has been successfully obtained.

Although bare MOF-253 does not absorb in the visible light region, MOF-253-Ru(dcbpy)$_2$ obtained by anchoring Ru moieties on MOF-253 via coordination with its open N,N′-chelating sites shows an absorption centered at 565 nm that extends to ca. 700 nm (Figure 2b). In comparison with

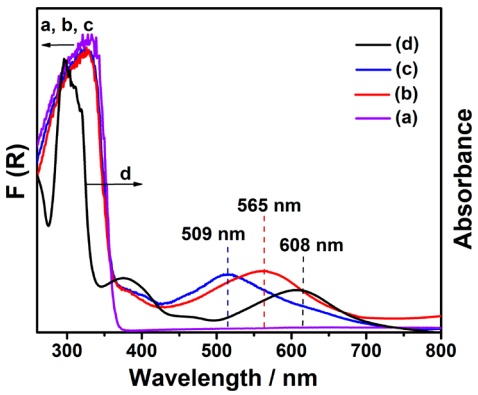

Figure 2. UV/vis DRS spectra of (a) MOF-253, (b) MOF-253-Ru(dcbpy)$_2$, and (c) Ru-MOF-253 and (d) UV−vis absorption spectrum of homogeneous Ru(dcbpy)$_2$Cl$_2$.

homogeneous Ru(dcbpy)$_2$Cl$_2$, which shows an absorption peak centered at 608 nm attributable to the Ru(II) to the LUMO of dcbpy, i.e. metal to ligand charge transfer (MLCT), the blue shift of the MLCT absorption observed over MOF-253-Ru(dcbpy)$_2$ again confirms the formation of coordinative bonds between Ru(II) and the N,N′-chelating sites in the MOF-253 framework.

Photocatalytic Reduction of CO_2 and Semidehydrogenation of THIQ over MOF-253-Ru(dcbpy)$_2$. The photocatalytic CO_2 reduction over MOF-253-Ru(dcbpy)$_2$ was initially carried out in DMF with the presence of THIQ under visible light, since DMF was previously demonstrated to be a good solvent for photocatalytic CO_2 reduction.[20] Unfortunately, almost negligible products of CO_2 reduction were detected after irradiation for 1 day, with only 1% of THIQ converted (Table 1, entry 1). Among the five solvents (DMF, H_2O, MeCN, DMSO, and THF) investigated (Table 1, entries 1−5), only MeCN showed an obvious activity for this reaction, with 6.4 μmol of formic acid and 0.8 μmol of CO produced, together with 10.8% of THIQ converted in 1 day (Table 1, entry 5). Almost no products were detected over irradiated bare MOF-253 or MOF-253-Ru(dcbpy)$_2$ without light irradiation, indicating that the reaction was truly induced by photocatalysis over MOF-253-Ru(dcbpy)$_2$.

The time-dependent product distribution of photocatalytic CO_2 reduction in the presence of THIQ over MOF-253-Ru(dcbpy)$_2$ in MeCN showed that the amount of formic acid and CO, the products of CO_2 reduction, increased continuously with irradiation, with 52.8 μmol of formic acid and 11.3 μmol of CO produced after irradiation for 5 days (Figure 3a). In the meantime, the amount of THIQ decreased continuously and 88.5% of THIQ was converted in 5 days, with a selectivity of 83.3% to DHIQ, the semidehydrogenation product of THIQ (Figure 3b, solid icon). No further conversion of CO_2 and THIQ was observed when MOF-253-Ru(dcbpy)$_2$ was removed from the reaction system after 3 days of irradiation (Figure 3b, hollow icon). In addition, ICP analysis of the filtrate revealed no detectable Ru, indicating that the reaction did occur over heterogeneous MOF-253-Ru-

DOI: 10.1021/acs.inorgchem.9b02593
Inorg. Chem. XXXX, XXX, XXX−XXX

Table 1. Photocatalytic CO_2 Reduction in the Presence of THIQ over the As-Obtained MOF-253-Ru(dcbpy)$_2$ under Different Reaction Conditions

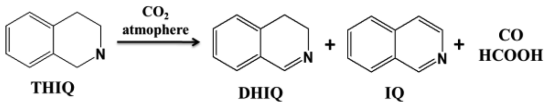

		yield, %				
entry[a]	solvent	DHIQ	IQ	THIQ conversn, %	CO, μmol	HCOOH, μmol
1	DMF	1.0		1.0	trace	
2	DMSO					
3	THF	3.6	0.4	3.9	trace	
4	H_2O					
5[b]	MeCN	10.3	0.4	10.8	0.8	6.4
6[c]	MeCN	29.3	2.1	32.1	2.1	21.3
7	MeCN	73.7	7.7	88.5	11.3	52.8
8[d]	MeCN					
9[e]	MeCN	78.3	8.0	91.1		
10[f]	MeCN	76.2	8.8	87.9	0.9	61.8
11[g]	MeCN			9.7	63.3	
12[h]	MeCN					
13[i]	MeCN	42.6	1.3	46.0	6.2	25.1

[a]Conditions unless specified otherwise: MOF-253-Ru(dcbpy)$_2$ (10 mg), MeCN (2 mL), THIQ (0.08 mmol), CO_2 (1 atm), 5 W white LED for 5 days of light irradiation. The evolution of quinolines was calculated by GC-FID, and the amounts of CO and HCOOH were obtained by GC-FID with a Ni reformer and IC, respectively. [b]1 day of light irradiation. [c]3 days of light irradiation. [d]Under an N_2 atmosphere. [e]Under an O_2 atmosphere. [f][Ru(dcbpy)$_3$]Cl$_2$ (2 mg) as the photocatalyst. [g]THIQ was replaced by TEOA. [h]MOF-253-Ru(CO)$_2$Cl$_2$ (10 mg) as the photocatalyst. [i]Ru-MOF-253 (10 mg) as the photocatalyst.

(dcbpy)$_2$. It is obvious that this reaction is a successful coupling of the photocatalytic CO_2 reduction with the photocatalytic dehydrogenation of THIQ over MOF-253-Ru(dcbpy)$_2$, since no formic acid and CO were detected when the reaction was carried out in the absence of THIQ. Similarly, no conversion of THIQ was observed when CO_2 was replaced by N_2 under otherwise similar conditions (Table 1, entry 8). However, the photocatalytic oxidation of THIQ occurred over MOF-253-Ru(dcbpy)$_2$ when O_2 was introduced into the system, giving an almost comparable conversion of THIQ (91.1%) and a yield of 78.8% to DHIQ (Table 1, entry 9). This result is in accordance with previous studies that photocatalytic oxidation of THIQ can be realized over homogeneous [Ru(bpy)$_3$]Cl$_2$.[17] In addition, the performance of MOF-253-Ru(dcbpy)$_2$ for CO_2 reduction in the presence of THIQ is comparable to that observed over homogeneous [Ru(dcbpy)$_3$]Cl$_2$, in which 61.8 μmol of formic acid and 0.9 μmol of CO together with a conversion of 87.9% to THIQ were obtained after 5 days of irradiation, indicating that the support of the Ru complex on the surface of the MOF did not sacrifice its performance (Table 1, entry 10).

Mechanism for CO_2 Reduction and THIQ Semi-dehydrogenation over MOF-253-Ru(dcbpy)$_2$. On the basis of previous studies, it is not difficult to propose the mechanism for the successful coupling of the photocatalytic CO_2 reduction with the dehydrogenation of THIQ to produce DHIQ over MOF-253-Ru(dcbpy)$_2$, as shown in Scheme 1. Similar to what occurs over homogeneous [Ru(bpy)$_3$]Cl$_2$, the MOF-supported Ru complex (MOF-253-Ru(dcbpy)$_2$) can also be excited to its excited state [MOF-253-Ru^{II}(dcbpy)]* (step 1).[35] The reductive quenching of the excited state by THIQ produces [MOF-253-Ru^{I}(dcbpy)], accompanied by the formation of a tetrahydroquinoline radical cation (steps 2 and 3). Such a reductive quenching pathway has been proposed in the photocatalytic dehydrogenation of THIQ to produce DHIQ over homogeneous [Ru(bpy)$_3$]Cl$_2$ due to a less positive potential of THIQ in comparison with that of E([Ru(bpy)$_3$]$^{2+}$*/[Ru(bpy)$_3$]$^{+}$). As is the case for [Ru(bpy)$_3$]-Cl$_2$, the tetrahydroquinoline radical cation releases another electron and two protons to form DHIQ, the semidehydrogenated product of THIQ (step 4). The as-formed [MOF-253-Ru^{I}(dcbpy)] acts as an active species for photocatalytic CO_2 reduction to recover MOF-253-Ru(dcbpy)$_2$ and produces formic acid and CO via a proton-coupled mechanism (step 5), which has already been well demonstrated in a series of homogeneous and supported Ru complexes containing bpy-based ligands.[8,14] Via a successful coupling of photocatalytic dehydrogenation of THIQ with reduction of CO_2 under visible light, not only can CO_2 be reduced to form the fuels (CO and formic acid) but also THIQ can be oxidized to produce DHIQ, an important starting material in the syntheses of pharmaceuticals, which makes the current reaction protocol economical and green.

As a stronger electron donor than THIQ, TEOA can also be used as the sacrificial agent in the current MOF-253-

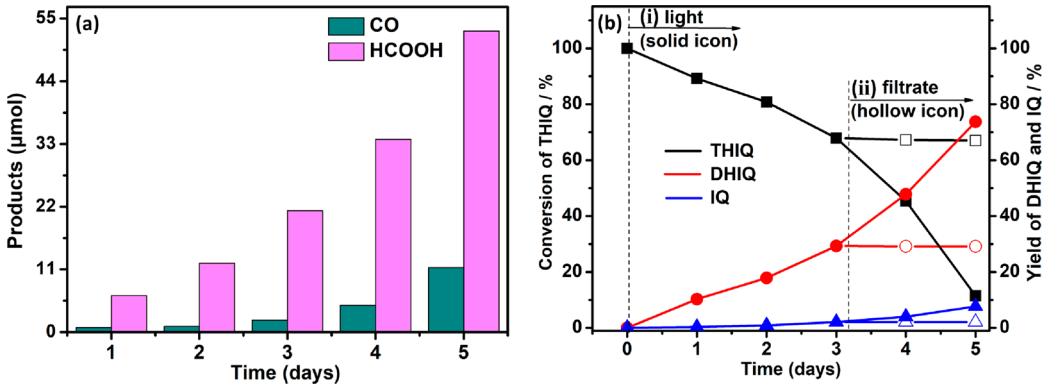

Figure 3. (a) Amount of CO and HCOOH produced after irradiated for different time over MOF-253-Ru(dcbpy)$_2$. (b) Time-dependent changes of THIQ conversion and the yields to the dehydrogenation products over irradiated MOF-253-Ru(dcbpy)$_2$: (i) after visible light irradiation (solid icons); (ii) after MOF-253-Ru(dcbpy)$_2$ was removed after irradiation for 3 days (hollow icons).

DOI: 10.1021/acs.inorgchem.9b02593
Inorg. Chem. XXXX, XXX, XXX−XXX

Scheme 1. Proposed Mechanism for Simultaneous Photocatalytic CO_2 Reduction and Dehydrogenation of THIQ under Visible Light

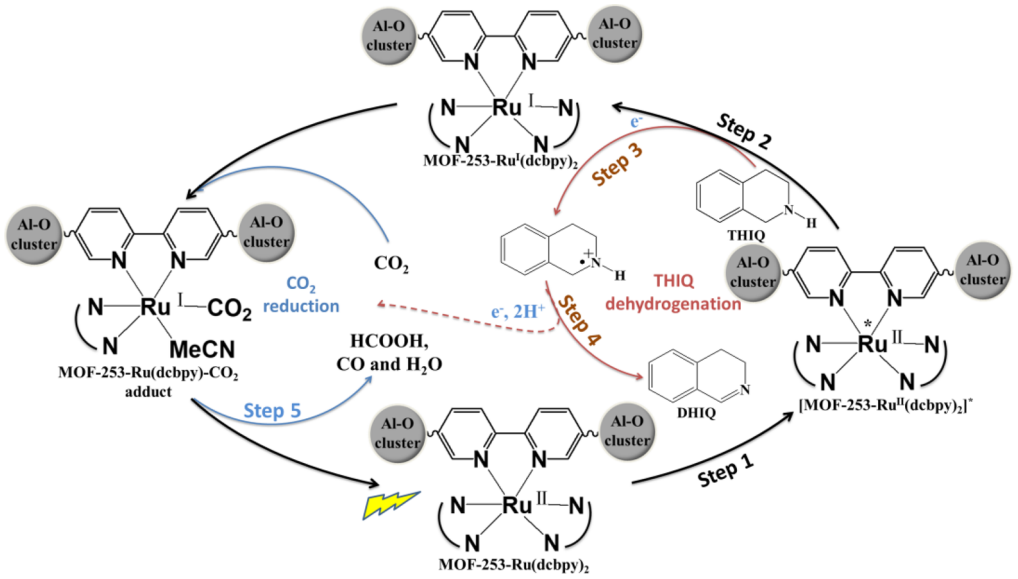

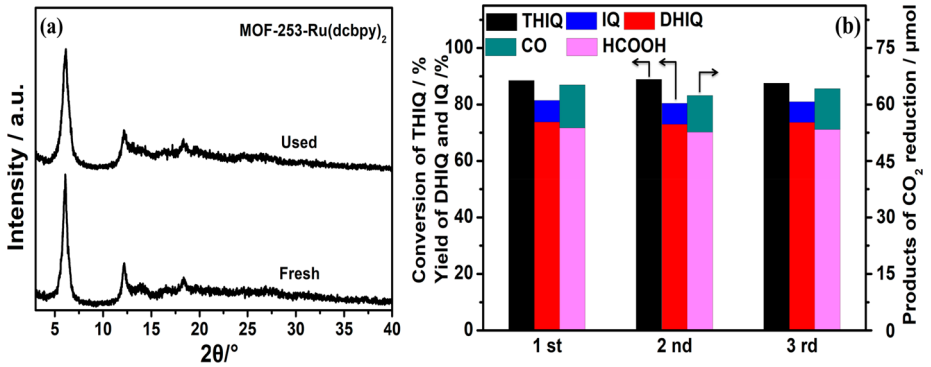

Figure 4. (a) XRD patterns of MOF-253-Ru(dcbpy)$_2$ before and after reaction. (b) Cycling use of MOF-253-Ru(dcbpy)$_2$ for the coupling of photocatalytic CO_2 reduction with dehydrogenation of THIQ.

Ru(dcbpy)$_2$ system for photocatalytic CO_2 reduction, with 63.6 μmol of HCOOH and 9.7 μmol of CO detected in 5 days, a better performance in comparison to that obtained in the presence of THIQ (Table 1, entry 11). However, although our previous studies revealed that photocatalytic CO_2 reduction was realized over MOF-253-Ru(CO)$_2$Cl$_2$, a similar MOF-253-supported Ru complex, in the presence of TEOA, it was not active for photocatalytic CO_2 reduction when THIQ was present (Table 1, entry 12). This indicates that the excited state of MOF-253-Ru(CO)$_2$Cl$_2$ can be quenched by TEOA but not THIQ, a result that is not unexpected since TEOA is a better electron donor than THIQ. This result indicates that the reductive quenching of the excited state by THIQ to produce the active Ru(I) intermediate is the prerequisite for the coupling of photocatalytic CO_2 with the dehydrogenation of THIQ.

Photocatalytic Reduction of CO_2 and Semidehydrogenation of THIQ over Ru-MOF-253. For comparison, a Ru-doped MOF-253 (Ru-MOF-253) obtained by reacting $AlCl_3 \cdot 6H_2O$ with a combination of dcbpy and [Ru(dcbpy)$_3$]Cl$_2$ via a mix-and-match strategy was also used for photocatalytic CO_2 reduction in the presence of THIQ under visible light (Figure S1b in the Supporting Information).[32] To exclude the influence of the amount of the catalytically active Ru species, an amount of Ru (6.4%) comparable to that over MOF-253-Ru(dcbpy)$_2$ was doped into MOF-253. Ru-MOF-253 also shows a comparable specific surface area (1047 $m^2 g^{-1}$). Similarly to MOF-253-Ru(dcbpy)$_2$, the XPS spectrum of Ru-MOF-253 in the Ru 3d region also shows a Ru $3d_{5/2}$ peak at a binding energy of 281.45 eV (Figure S5 in the Supporting Information). However, unlike Ru moieties in MOF-253-Ru(dcbpy)$_2$ which coordinate to MOF-253 only via N,N′-open sites in the dcbpy ligand in MOF-253, Ru moieties in the doped Ru-MOF-253 interact more strongly with the framework of MOF-253, since [Ru(dcbpy)$_3$]Cl$_2$ acts as a metalloligand to take part in the formation of the framework of MOF-253. This can be evidenced from their slightly different FT-IR and UV−vis DRS spectra. The C═O vibrational stretch in Ru-MOF-253 occurs at 1695 cm^{-1}, which slightly shifts to a higher wavenumber in comparison with that in MOF-253-Ru(dcbpy)$_2$ (1690 cm^{-1}) (Figure 1b). In addition, the MLCT in Ru-MOF-253 was blue-shifted to 509 nm with respect to that in MOF-253-Ru(dcbpy)$_2$ (565 nm), ascribable to a increase in the π^* energy of the dcbpy ligand when it takes part in the formation of the framework of MOF-253 (Figure 2c).[36] Ru-MOF-253 showed inferior photocatalytic activity under otherwise similar conditions in comparison with MOF-253-Ru(dcbpy)$_2$. Only 25.1 μmol of formic acid and 6.3 μmol of

DOI: 10.1021/acs.inorgchem.9b02593
Inorg. Chem. XXXX, XXX, XXX−XXX

CO were produced, together with 46% of THIQ converted after irradiation for 5 days (Table 1, entry 13). It is obvious that MOF-253-Ru(dcbpy)$_2$ is more active than the doped Ru-MOF-253 even though both catalysts contain almost similar catalytically active Ru moieties and have comparable specific surface areas. This result is not difficult to understand if we consider that the photocatalytic CO_2 reduction over the bpy-containing Ru complexes involves the breaking of one of the Ru−N bonds to create an empty site for CO_2 insertion. In comparison with supported MOF-253-Ru(dcbpy)$_2$, the stronger interaction between Ru moieties and the framework in Ru-MOF-253 leads to a stronger Ru−N bond, which is more difficult to break for CO_2 insertion in comparison with that in MOF-253-Ru(dcbpy)$_2$. Therefore, supported MOF-253-Ru-(dcbpy)$_2$ is more efficient in photocatalytic CO_2 reduction and THIQ dehydrogenation than Ru-MOF-253. This suggests that the supported molecular complexes obtained by coordination with the open coordination sites in the MOFs are superior to that fabricated by the mix-and-match strategy in maintaining the performance of their homogeneous counterpart.

The as-obtained supported MOF-253-Ru(dcbpy)$_2$ is stable during the photocatalytic reaction, as evidenced from its unchanged XRD patterns after the photocatalytic reaction (Figure 4a). In addition, no obvious loss of the photocatalytic performance was observed after three cycling uses (Figure 4b). The superior recyclability of MOF-253-Ru(dcbpy)$_2$ in comparison with its homogeneous counterpart is an inherent advantage of being a heterogeneous catalyst.

CONCLUSION

In summary, MOF-253-Ru(dcbpy)$_2$, a surface-constructed Ru complex, shows photocatalytic performance for the simultaneous CO_2 reduction to produce formic acid and CO as well as semidehydrogenation of THIQ to obtain DHIQ under visible light. The surface-supported MOF-253-Ru(dcbpy)$_2$ achieved a better performance than Ru-doped Ru-MOF-253 fabricated via a mix-and-match strategy, indicating that the use of the open coordination sites in the MOFs for the direct construction of a surface-supported complex is a superior strategy in obtaining MOF-supported homogeneous complexes without sacrificing their performance. This strategy highlights the great potential of using MOFs as a platform for the fabrication of multifunctional heterogeneous photocatalytic systems. The coupling of photocatalytic CO_2 reduction with highly selective dehydrogenation of organics represents an economical and green strategy in CO_2 conversion.

ASSOCIATED CONTENT

Supporting Information

The Supporting Information is available free of charge at https://pubs.acs.org/doi/10.1021/acs.inorgchem.9b02593.

XRD pattern of the MOF-253 and MOF-253-Ru-(dcbpy)$_2$ obtained by a solvothermal method, syntheses of MOF-253-Ru(dcbpy)$_2$ and Ru-MOF-253, N_2 adsorption/desorption isotherms (77 K) of MOF-253-Ru-(dcbpy)$_2$ and MOF-253, and the XPS spectra of MOF-253, MOF-253-Ru(dcbpy)$_2$, and Ru-MOF-253 (PDF)

AUTHOR INFORMATION

Corresponding Author

*E-mail for Z.L.: zhaohuili1969@yahoo.com.

ORCID

Zhaohui Li: 0000-0002-3532-4393

Notes

The authors declare no competing financial interest.

ACKNOWLEDGMENTS

This work was supported by NSFC (21872031 and U1705251). Z.L. thanks the Award Program for Minjiang Scholar Professorship for financial support.

REFERENCES

(1) Rogelj, J.; Forster, P. M.; Kriegler, E.; Smith, C. J.; Seferian, R. Estimating and tracking the remaining carbon budget for stringent climate targets. *Nature* **2019**, *571*, 335−342.

(2) Mardani, A.; Streimikiene, D.; Cavallaro, F.; Loganathan, N.; Khoshnoudi, M. Carbon dioxide (CO_2) emissions and economic growth: A systematic review of two decades of research from 1995 to 2017. *Sci. Total Environ.* **2019**, *649*, 31−49.

(3) Liu, C. J. How do you explain the importance of CO_2 utilization? *Greenhouse Gases: Sci. Technol.* **2017**, *7*, 397−398.

(4) Liang, J.; Huang, Y.-B.; Cao, R. Metal-organic frameworks and porous organic polymers for sustainable fixation of carbon dioxide into cyclic carbonates. *Coord. Chem. Rev.* **2019**, *378*, 32−65.

(5) Artz, J.; Muller, T. E.; Thenert, K.; Kleinekorte, J.; Meys, R.; Sternberg, A.; Bardow, A.; Leitner, W. Sustainable conversion of carbon dioxide: An integrated review of catalysis and life cycle assessment. *Chem. Rev.* **2018**, *118* (2), 434−504.

(6) Chang, X.; Wang, T.; Gong, J. CO_2 photo-reduction: insights into CO_2 activation and reaction on surfaces of photocatalysts. *Energy Environ. Sci.* **2016**, *9*, 2177−2196.

(7) Chen, Y.; Wang, D.; Deng, X.; Li, Z. Metal-organic frameworks (MOFs) for photocatalytic CO_2 reduction. *Catal. Sci. Technol.* **2017**, *7*, 4893−4904.

(8) Yamazaki, Y.; Takeda, H.; Ishitani, O. Photocatalytic reduction of CO_2 using metal complexes. *J. Photochem. Photobiol., C* **2015**, *25*, 106−137.

(9) Dean, J. A. *Lange's Handbook of Chemistry*; McGraw-Hill: New York, 1999.

(10) Sahara, G.; Ishitani, O. Efficient photocatalysts for CO_2 reduction. *Inorg. Chem.* **2015**, *54*, 5096−104.

(11) Kuramochi, Y.; Ishitani, O.; Ishida, H. Reaction mechanisms of catalytic photochemical CO_2 reduction using Re(I) and Ru(II) complexes. *Coord. Chem. Rev.* **2018**, *373*, 333−356.

(12) Kumar, B.; Llorente, M.; Froehlich, J.; Dang, T.; Sathrum, A.; Kubiak, C. P. Photochemical and photoelectrochemical reduction of CO_2. *Annu. Rev. Phys. Chem.* **2012**, *63*, 541−69.

(13) Voyame, P.; Toghill, K. E.; Mendez, M. A.; Girault, H. H. Photoreduction of CO_2 using $[Ru(bpy)2(CO)L]^{n+}$ catalysts in biphasic solution/supercritical CO_2 systems. *Inorg. Chem.* **2013**, *52*, 10949−57.

(14) Sun, D.; Gao, Y.; Fu, J.; Zeng, X.; Chen, Z.; Li, Z. Construction of a supported Ru complex on bifunctional MOF-253 for photocatalytic CO_2 reduction under visible light. *Chem. Commun.* **2015**, *51*, 2645−8.

(15) Scott, J. D.; Williams, R. M. Chemistry and biology of the tetrahydroisoquinoline antitumor antibiotics. *Chem. Rev.* **2002**, *102*, 1669−1730.

(16) Hao, M.; Deng, X.; Xu, L.; Li, Z. Noble metal Free MoS_2/$ZnIn_2S_4$ nanocomposite for acceptorless photocatalytic semi-dehydrogenation of 1,2,3,4-tetrahydroisoquinoline to produce 3,4-dihydroisoquinoline. *Appl. Catal., B* **2019**, *252*, 18−23.

(17) Chen, S.; Wan, Q.; Badu-Tawiah, A. K. Picomole-scale real-time photoreaction screening: discovery of the visible-light-promoted dehydrogenation of tetrahydroquinolines under ambient conditions. *Angew. Chem., Int. Ed.* **2016**, *55*, 9345−9349.

(18) Bock, C. R.; Connor, J. A.; Gutierrez, A. R.; Meyer, T. J.; Whitten, D. G.; Sullivan, B. P.; Nagle, J. K. Estimation of excited-state

DOI: 10.1021/acs.inorgchem.9b02593
Inorg. Chem. XXXX, XXX, XXX−XXX

redox potentials by electron-transfer quenching. Application of electron-transfer theory to excited-state redox processes. *J. Am. Chem. Soc.* **1979**, *101*, 4815−4824.
(19) Prier, C. K.; Rankic, D. A.; Macmillan, D. W. C. Visible light photoredox catalysis with transition metal complexes: applications in organic synthesis. *Chem. Rev.* **2013**, *113*, 5322−5363.
(20) Lehn, J. M.; Ziessel, R. Photochemical reduction of carbon dioxide to formate catalyzed by 2,2' -bipyridine- or 1,10-phenanthroline-ruthenium(II) complexes. *J. Organomet. Chem.* **1990**, *382*, 157−173.
(21) Dhakshinamoorthy, A.; Li, Z.; Garcia, H. Catalysis and photocatalysis by metal organic frameworks. *Chem. Soc. Rev.* **2018**, *47*, 8134−8172.
(22) Jiao, L.; Wang, Y.; Jiang, H. L.; Xu, Q. Metal-organic frameworks as platforms for catalytic applications. *Adv. Mater.* **2018**, *30*, No. 1703663.
(23) Cohen, S. M.; Zhang, Z.; Boissonnault, J. A. Toward "metalloMOFzymes": Metal-organic frameworks with single-site metal catalysts for small-molecule transformations. *Inorg. Chem.* **2016**, *55*, 7281−7290.
(24) Niu, Z.; Bhagya Gunatilleke, W. D. C.; Sun, Q.; Lan, P. C.; Perman, J.; Ma, J.-G.; Cheng, Y.; Aguila, B.; Ma, S. Metal-organic framework anchored with a lewis pair as a new paradigm for catalysis. *Chem.* **2018**, *4*, 2587−2599.
(25) Drake, T.; Ji, P.; Lin, W. Site isolation in Metal-organic frameworks enables novel transition metal catalysis. *Acc. Chem. Res.* **2018**, *51*, 2129−2138.
(26) Dhakshinamoorthy, A.; Asiri, A. M.; Garcia, H. Formation of C-C and C-heteroatom bonds by C-H activation by metal organic frameworks as catalysts or supports. *ACS Catal.* **2019**, *9*, 1081−1102.
(27) Deng, X.; Albero, J.; Xu, L.; Garcia, H.; Li, Z. Construction of a stable Ru-Re hybrid system based on multifunctional MOF-253 for efficient photocatalytic CO_2 reduction. *Inorg. Chem.* **2018**, *57*, 8276−8286.
(28) Zhou, T.; Du, Y.; Borgna, A.; Hong, J.; Wang, Y.; Han, J.; Zhang, W.; Xu, R. Post-synthesis modification of a metal-organic framework to construct a bifunctional photocatalyst for hydrogen production. *Energy Environ. Sci.* **2013**, *6*, 3229.
(29) Fei, H.; Cohen, S. M. A robust, catalytic metal-organic framework with open 2,2'-bipyridine sites. *Chem. Commun.* **2014**, *50*, 4810−2.
(30) Bloch, E. D.; Britt, D.; Lee, C.; Doonan, C. J.; Uribe-Romo, F. J.; Furukawa, H.; Long, J. R.; Yaghi, O. M. Metal insertion in a microporous metal-organic framework lined with 2,2'-bipyridine. *J. Am. Chem. Soc.* **2010**, *132*, 14382−14384.
(31) Eskelinen, E.; Luukkanen, S.; Haukka, M.; Ahlgrén, M.; Pakkanen, T. A. Redox and photochemical behaviour of ruthenium-(II) complexes with H_2dcbpy ligand (H_2dcbpy = 2,2'-bipyridine-4,4'-dicarboxylic acid). *J. Chem. Soc., Dalton Trans.* **2000**, No. 16, 2745−2752.
(32) Wang, C.; Xie, Z.; deKrafft, K. E.; Lin, W. Doping metal-organic frameworks for water oxidation, carbon dioxide reduction, and organic photocatalysis. *J. Am. Chem. Soc.* **2011**, *133*, 13445−54.
(33) Ni, Z.; Masel, R. I. Rapid production of metal-organic frameworks via microwave-assisted solvothermal synthesis. *J. Am. Chem. Soc.* **2006**, *128*, 12394−5.
(34) Falaras, P. Synergetic effect of carboxylic acid functional groups and fractal surface characteristics for efficient dye sensitization of titanium oxide. *Sol. Energy Mater. Sol. Cells* **1998**, *53*, 163−175.
(35) Condie, A. G.; González-Gómez, J. C.; Stephenson, C. R. J Visible-light photoredox catalysis: aza-Henry reactions via C-H functionalization. *J. Am. Chem. Soc.* **2010**, *132*, 1464−1465.
(36) Kalyanasundaram, K.; GräTzel, M. Applications of functionalized transition metal complexes in photonic and optoelectronic devices. *Coord. Chem. Rev.* **1998**, *177*, 347−414.

DOI: 10.1021/acs.inorgchem.9b02593
Inorg. Chem. XXXX, XXX, XXX−XXX